Proceedings of the 7th International Conference on HydroScience and Engineering

Philadelphia, USA September 10-13, 2006 (ICHE 2006)

ISBN: 0977447405

Drexel University

College of Engineering

DRAG REDUCTION ON SALTATING SEDIMENT IN SHALLOW FLOW

Shyam N Prasad[1], S Madhusudana Rao[2] and Mathias J M Römkens[3]

ABSTRACT

Laboratory flume experiments of shallow overland flow with sediments consisting of sand particles of sizes (1000-1400 μm) and (600- 850 μm) and fine particles of sand (74-125 μm) revealed several features similar to gravity driven granular flow experiments with glass beads [Prasad *et al.* (2000)]. In the saltating flow regime the particle velocity was measured by cross-correlating signals obtained with twin photonic probes and particle concentrations by pre-calibrated single probe signals. In the very low particle concentration range, particle velocity showed an increased trend followed by a decreased trend at larger concentration values. A simple model was developed for the particles transport in water that showed drag reduction by so called "drafting". This "drafting" model is based on the superposition principle of two flow fields. First the drag coefficient is computed for the case of a single particle and the second part consists of a similar coefficient due to the flow field behind the leading particle. Thus, for a row of infinite number of spherical particles of diameter, d_s, equally spaced at a distance, s, (center to center), the ratio of the drag coefficients (multiple to single particles) is found to be $(1 - c\alpha^2)$ where α is the linear concentration, d_s/s and c (a constant) depends on the particle Reynolds number.

1. INTRODUCTION

Drag reduction has been observed in channel flows when clay particles in low concentrations are present. Previous studies [Li and Gust (2000) & Graf and Cellino (1999)] have discovered increased magnitudes of velocity profiles associated with decreases in bed shear stresses (expressed as shear velocity) in the presence of suspended particles. Measurements of velocity profiles and of the shear velocity in the viscous sub-layer indicate significant thickening of the inner wall layer and dampening of turbulence in the viscous sub-layer. These effects become stronger for higher concentrations and lower flow strength, suggesting that they are responsible for drag reduction in open channel flows with particle suspension.

Although these studies predict the equilibrium hydraulic conditions of suspended sediments in open channel flows through the coupled phenomena of resistance to flow and transport processes, studies of particle dynamic parameters such as grain velocities or solid concentrations are lacking. Our

[1] Professor, Department of Civil Engineering, University of Mississippi, University, MS 38677, USA (cvprasad@olemiss.edu)
[2] Research Assistant Professor, Department of Civil Engineering, University of Mississippi, University, MS 38677, USA
[3] Director, ARS/USDA National Sedimentation Laboratory, Oxford, MS 38655, USA

present study therefore focuses on these types of measurements. This research started with optical (photonic) probe measurements of particle velocity and concentrations in saltating conditions in a laboratory flume under different hydrodynamic conditions. Solid concentrations were obtained by determining the fraction of the illuminated area under the optical probe covered by passing grains. Particle velocities were determined from the cross-correlation values of twin photonic probe data. It was found that the velocity increases initially with increasing solid concentration. The velocity reaches a maximum until a critical stage is reached when particle collisions become significant and the transport mode changes from saltation to a certain organized bed state. A significant energy loss due to collisions reduces the particle velocities and a drastic reduction in the sediment transport rates may result. These measurements were performed for various particle sizes and flow rates.

The increase in particle velocity with concentration was rather unexpected and appears to be the result of the net effect of at least two distinct mechanisms. Since there is a redistribution of the near-wall flow field, similar to the case of transport of suspended material, the resulting increase in the flow velocity will also increase the particle velocity. But the more interesting aspect of increased particle velocities is associated with the effect on particles that follow each other. There are well known observations that in nature bodies (such as birds, fishes and ducks) move in a group to conserve energy. A rather simple model is developed in this article that shows drag reduction by so called "drafting". This "drafting" effect model is based on the superposition principle of two flow fields. First the drag coefficient is computed for the flow field of a single particle and the second part consists of similar, negative coefficient due to the flow field behind the leading particles. Thus, for a row of infinite number of spherical particles of diameter, d_s, equally spaced at a distance, s, (center to center), the ratio of the drag coefficients (multiple to single particles) is found to be $(1-c\alpha^2)$ where α is the linear concentration, d_s/s and c depends on particle Reynolds number. The flow field behind the spherical particle is obtained either by Stokes or Oseen analysis. In particular, the Stokes solution leads to $c = 3\pi^2/32$. This article discusses the details of these analysis as well as experimentally determined values for various cases.

2. EXPERIMENTAL SETUP

A schematic diagram of the experimental set-up is shown in figure 1. The test section consists of a 700 cm x 10.7cm x 4.4 cm deep rectangular open aluminum channel with an inclination < 1°. The surface is conditioned by metallic spray paint. A traverse mechanism allows the attainment of the desired slope of the channel relevant to the bottom reference surface. The channel is uniformly supported at selected locations to avoid any axis-wise deflection due to its self weight. Tap water enters at the upstream end through a surge tank, regulating valve, and an intermediate tank. The surge tank provides a steady supply of water to the intermediate tank with fixed pressure head thus eliminating any pressure fluctuation in the water source line. The desired water flow rate can be attained by means of the regulating valve. Experiments are performed by keeping the valve opening constant and by varying the solids feed rate into the water stream. The channel entrance arrangement together with a set of divergent baffles in the intermediate tank ensures smooth flow of water. Sand granules of two large sizes (poly-dispersed) namely, coarse (1000-1400 μm) and medium (600-850 μm) sized sand; fine size white sand (74-125 μm), and spherical glass beads (600-1000 μm) (The physical properties are listed in Table 1) are observed under various hydraulic conditions with the 'Fr_l' ($U_f^2/g.h$) number having a maximum value of about 2. These granules are entrained into the water stream at about 50 cm from the upstream end by using a vibrating hopper and feeder arrangement. The desired solids feed rate can be obtained by adjusting the clearance between the hopper with the feeder, frequency, and amplitude of vibrations and the feeder inclination. The

downstream boundary ensured minimum washing of solids, hence simulating an infinitely long channel. The transported sand granules at the drain end are filtered and recycled after drying. Particle velocities are estimated by cross-correlating the reflected light signals from the solids passing through the field of vision of the twin Photonic probes located at about 427.5cm from the upstream end. The probes are mounted on a solid block (figure 2) and a micrometer allows clearance adjustment between the sensing surface of the probe with the channel bottom surface where a very thin (~0.0025 inches) reflective tape is affixed. Two optical probe models 2020R and 2125H (MTI Instruments Inc., NY)) with sensing diameters 2.5mm and 8mm respectively together with a dynamic signal analyzer (HP35665A) are used for the online recording of data on particle velocity and concentration. The sensor probe consists of an emitting source and receiving optics mounted into a steel sheath which is connected to the signal analyzer by means of fiber optics. When the emitted light from the source optics is obstructed by a reflective surface, a portion of the reflective light is detected by the receiving optics. The signal response of detecting optics depends on the magnitude and nature of obstruction and on the distance between the probe surface and the reflective object. The probes are calibrated for the solids concentration measurements in a water column with known amount of solid grains. When the probes are completely covered by solid grains the concentration upper bound is assigned a value 1, conversely when there are no solid grains, under the probe light exposure area the lower bound solids concentration value is set at 0. The signal information from the small probe diameters (2020R) represents data from distinct particles whereas the large diameter probes (2125H) capture density pattern propagation of solid clouds. Solid concentration measurements from the large probe diameters are closer to the global average value. The particle velocity is estimated by cross-correlating the data from the twin-probe recordings.

The time-averaged particle concentration ($\overline{\alpha}_t$) was found by averaging $\alpha_s(z, t)$ over a time period T (typically 60 s and 500 ms for concentration and velocity measurements respectively): and the time-average value of $\overline{\alpha}_s(z,t)$ is denoted by $\langle\alpha\rangle(z)$:

$$\langle\alpha\rangle(z)=\frac{1}{T}\int \alpha_s(z,t)dt \tag{1}$$

Here $\alpha_s(z,t)$ is the concentration value corresponding to the sensing area of probes at the axial location 'z' and time 't'.

The cross-correlation coefficient, C(*d*), where *d* denotes the delay time, was then computed as

$$C(d) = \frac{1}{T}\int_0^T \left(\alpha_s(z_1,t)-\langle\alpha\rangle(z_1)\right)\left(\alpha_s(z_2,t+d)-\langle\alpha\rangle(z_2)\right)\,dt \tag{2}$$

Here, z_1 and z_2 refer to upstream and downstream probes respectively, and *d* was taken to be positive. The dominant pattern propagation velocity, U_p, was estimated from $U_p = L/D$, where L is the axial distance between the two Photonic sensors and D is the value of *d* at which *C*(*d*) assumes the largest value. U_p estimated in this manner is clearly based on sensing area averages.

Table 1 Physical properties of material

Material	Diameter (d_s), μm	Density (ρ_s), kg/m^3	Packing factor (F_p)
Coarse sand	1000-1400	2,516	0.65
Medium sand	600-850	2,667	0.61
Glass beads	600-1000	1,519	0.68
White sand	74-125	2,700	-

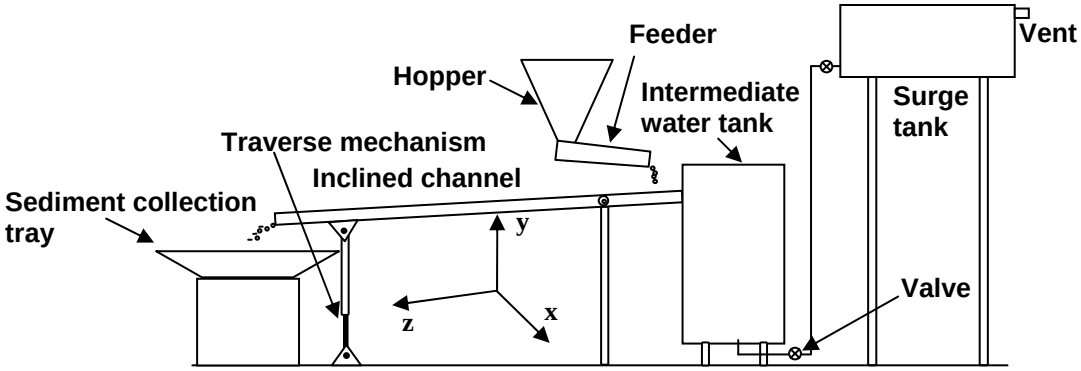

Figure 1 Schematic diagram of the experimental set-up.

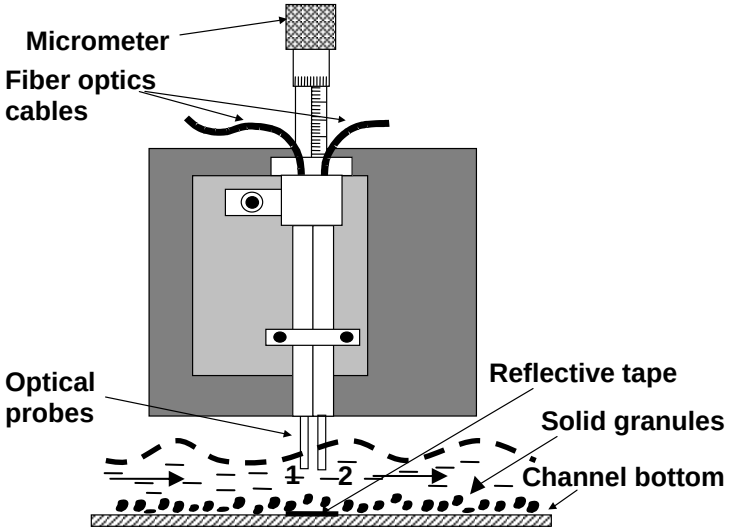

Figure 2 Twin plane arrangement of Photonic probes with module, upstream and downstream probes are labeled with numbers 1, 2 respectively.

3. SEDIMENT TRANSPORT IN SHALLOW OVERLAND FLOW

When a small amount of sand of size 600-850 μm (referred to "medium sand") or 1000-1400 μm (referred to "coarse sand") are added into the water stream the dominant mode of grain transport is saltation. As the grain addition rate increases gradually the mean free path distance of the saltating sand decreases and may lead to small clustering which with further increase evolve into small scale structures such as evenly spaced stripes and large scale structures resembling meanders and alternate bars. Figure 3 describes such an experiment showing the temporal evolution of various bed forms for the medium sand. The sand addition rate was 168.9 g/min and the water discharge rate was 15.7 l/min. Similar experiments with fine size sands, however, of size 74-125 μm (figure 4) showed distinctly different bed features such as Taylor streaks (low solids addition rates) and Barcan dunes (with relatively large solids addition rate). One of the significant factors controlling the formation of a structured bed appears to be the dependence of particle velocity on particle concentration. The following section reports data on particle velocity in the saltation phase.

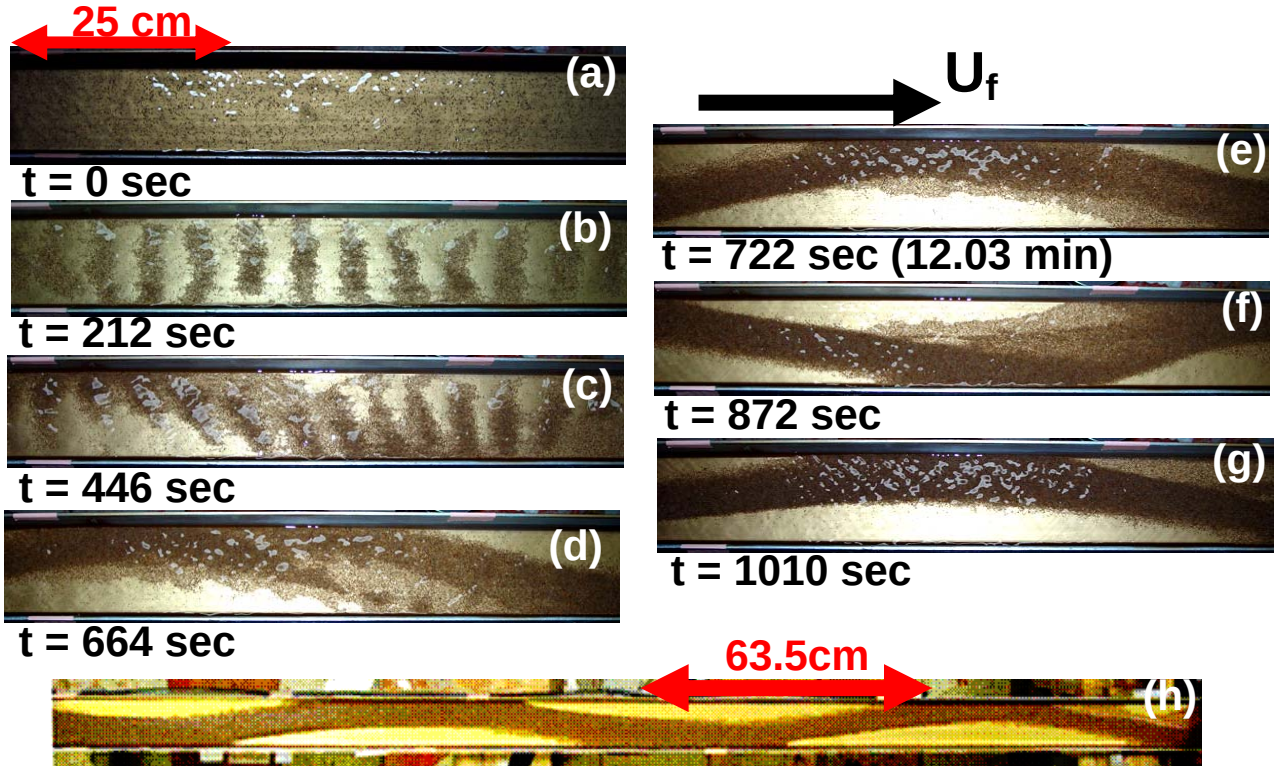

Figure 3 (a) – (g) Grain structure formations and its development (all the figures correspond to the same scale (camera placed at a fixed location). (h) – Fully developed meander structure (m_t = 10.2 g/min). Particle size, d_s = 600 – 850 µm; Water flow rate, q_l = 15.7 l/min (Fr_l = 1.45); solids feed rate is constant, m_s = 168.9 g/min.

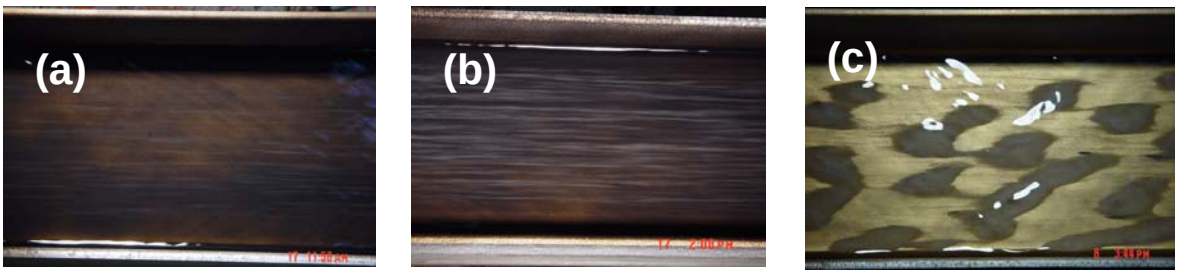

Figure 4 Bed structures with white sand (d_s = 74-125 µm); Water flow rate, q_l = 24 l/min (a) Taylor streaks with solids fee rate, m_s = 10.1 g/min and feed rate, m_t = 8.58 g/min (b) Taylor streaks with solids feed rate, m_s = 51.4 g/min while the corresponding transport rate, m_t = 26.5 g/min (c) Barcan dunes with solids feed rate, m_s = 67.9 g/min, while the transport rate is at 22.0 g/min.

3.1 Particle Velocity and Concentration Measurements

Figure 5 shows the time-averaged solid concentration $\overline{\alpha_s}$ values obtained from single probe measurements, as a function of the measured grain velocity obtained from the twin-probe data. Data shown in figure 5 are for the three particle sizes of, medium sand, coarse sand, and spherical glass beads, respectively, and two water flow rates q_l = 15.7 l/min (Fr_l = 1.45) and q_l = 21.6 l/min (Fr_l = 1.92). An increase in Froude number from 1.45 to 1.92 resulted in grain velocities about 2 times higher for a given solid concentration value. Here two mechanisms are worth noting. Firstly, as the

water flow rate increases the associated kinetic energy increases. Accordingly, the increased stress transmission from water to solids would lead to a greater saltation of the solid particles. Secondly, as the Froude number increases the turbulent eddies from the bed surface would also increase further the saltation activities of the sediments. The suspended particles would tend to move faster. The two-fold increase in grain velocity continues until the solid concentration reaches a critical value. However, as shown by Francis (1973), turbulence has limited, if any, influence on the saltation mechanism. The experimental observations indicates consistently an initial increase followed by a decrease in the grain velocity with increasing solid concentration. The explanation for this observation may be due to the modulation of turbulence by the presence of solid grains and a reduction of the drag coefficient due to "drafting". From epoxy-coated hot-film sensor measurements on clay suspensions, Li and Gust (2000) also observed particle drag reduction with relatively large solid concentrations. In our experiments, this phenomenon is consistently observed for the three particle sizes that were used. Spherical particles showed a higher grain velocity compared to the poly-dispersed sand particles. This is attributed to the smaller frictional resistance of the rolling spherical particles, with smooth surfaces. However, the grain velocities among the poly-dispersed sand particles seem to suggest a different trend. Figure shows that for a water flow rate of 15.7 l/min, the grain velocities with coarse sand are larger as compared to the medium sand particles up to a concentration value of about 0.007. But for solid concentration values above 0.007, the coarse particles seem to be already transitioning from saltation into organised state, in constrast to the medium sand partciles which are still in saltating mode.

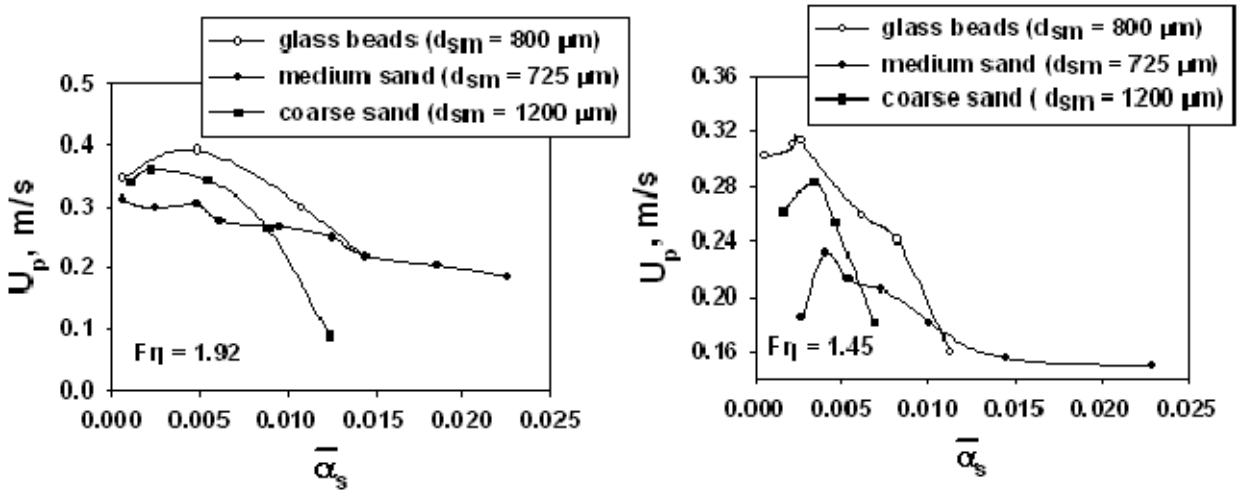

Figure 5 Measured velocity vs. concentration relationships for glass beads, coarse and medium sized sand for two hydraulic conditions ($Fr_l = 1.92$ and $Fr_l = 1.45$)

4. DRAG REDUCTION ANALYSIS

We consider a series of particles (spherical) of diameter, d_s equally spaced and moving with constant velocity u_p in a stream where the fluid velocity at the elevation of the particles is u_f (figure 6).

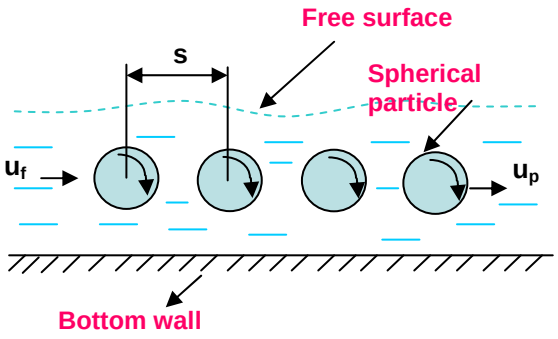

Figure 6 A simple arrangement of particles for the drag reduction model

The center-center distance between the particles is s. The slip velocity u_0 is given by

$$u_0 = u_f - u_p \tag{3}$$

The drag force on a particle is given by

$$F_D = C_D u_0^{\,2} \tag{4}$$

where C_D is the drag coefficient. The viscous drag on the particle is given by Stokes approximation which is based on the continuum analysis of linear fluid motion. The analysis involves determining the stream function ψ which for axi-symmetric flow is given by

$$\psi = \frac{1}{4} u_0 \left(2r^2 - \frac{3}{2} d_s r + \frac{d^3}{8} \frac{1}{r} \right) \sin^2 \theta \tag{5}$$

The velocity field results into

$$u_r = u_0 \left(\frac{3}{4} \frac{d_s}{r} - \frac{{d_s}^3}{16 r^3} \right) \cos\theta \tag{6}$$

$$u_\theta = u_0 \left(2 - \frac{3}{8} \frac{d_s}{r} - \frac{{d_s}^3}{32 r^3} \right) \sin\theta \tag{7}$$

where u_r and u_θ are the radial and tangential components of velocity and r is the radial distance and θ is the angle which the radius vector makes with the axis of flow. The viscous drag on the particle is given by

$$D_* = 3\pi\mu\, u_0 d_s \tag{8}$$

where μ is the coefficient of viscosity.

The above analysis does not include inertial effect of fluid motion which may be significant for moderate Reynolds number especially in the wake region away from the particle center. An improved approximation in the far region may be obtained by Oseen's expression in terms of Reynolds number R given by $u_0 d_s/\mu$. The analysis leads to the following expression of the stream function

$$\psi = \frac{u_0 {d_s}^2}{16} (r-1)^2 \sin^2\theta \left[\left(1 + \frac{3R}{8} \right) (2+r)^{-1} - \frac{3R}{8} \left(2 + \frac{1}{r} + \frac{1}{r^2} \right) \cos\theta \right] \tag{9}$$

which leads to the following expression for the radial velocity field

$$u_r = \frac{u_0 {d_s}^2}{16}\frac{(r-1)^2}{r^2}\cos\theta\left[\left(1+\frac{3R}{8}\right)(2+r)^{-1} - \frac{3R}{8}\left(2+\frac{1}{r}+\frac{1}{r^2}\right)\cos\theta\right] + \frac{3u_0 {d_s}^2 R}{128 r^2}(r-1)^2\sin^2\theta\left(2+\frac{1}{r}+\frac{1}{r^2}\right) \quad (10)$$

Similary, when first order correction to drag on the particles is considered, the drag is given by

$$D_{**} = 3\pi\mu\, u_0 d_s\left(1+\frac{3R}{8}\right) \quad (11)$$

The velocity distribution in the wake region of the particles is given from (6) by substituting θ = 0 which yields

$$u_r = \frac{u_0 d_s}{4r}\left(3-\frac{{d_s}^2}{4r^2}\right) \quad (12)$$

In order to see the "drafting" effect by a group of particles, we consider first two particles moving together with a separation distance s. The reduction in drag on the follower particle may be estimated by the superposition principle of their flow fields. The first part is the drag on the single particle which is given by

$$F_{D1} = C_D {u_0}^2 \quad (13)$$

whereas the second part is due to the flow field behind the leading particle and will have opposite sign. The wake velocity at the center of the follower is obtained from (12) by substituting r = s which leads to

$$u^* = \frac{u_0}{4}\alpha\left(3-\frac{\alpha^2}{4}\right) \quad (14)$$

where α is the linear concentration given by

$$\alpha = \frac{d_s}{s} \quad (15)$$

Thus the net drag on the follower is given by

$$F_{D2} = C_D\left({u_0}^2 - {u_0}^{*2}\right) \quad (16)$$

when α <<1, equation (14) yields

$$F_{D2} = C_D {u_0}^2\left(1-\frac{9}{16}\alpha^2\right) \quad (17)$$

when a group of three particles move together the drag on the last (3rd) particle will be

$$F_{D3} = C_D {u_0}^2\left[1-\frac{9}{16}\left(1+\frac{1}{2^2}\right)\alpha^2\right] \quad (18)$$

For a group of N particles equally spaced the drag on the last particle will be

$$F_{DN} = C_D {u_0}^2\left[1-\frac{9}{16}\left(1+\frac{1}{2^2}+\frac{1}{3^2}+\cdots\frac{1}{N^2}\right)\alpha^2\right] \quad (19)$$

This leads to the drag on particles uniformly spaced moving in the stream

$$F_{DN} = C_D {u_0}^2\left[1-\frac{9}{16}\frac{\pi^2}{6}\alpha^2\right] \quad (20)$$

The drag reduction coefficient, k is given by

$$k = \frac{F_{DN}}{C_D u_0^{\,2}} = \left(1 - \frac{3\pi^2}{32}\alpha^2\right) \qquad (21)$$

The above formula clearly shows that the net drag on particles reduces with concentration, α. Our experimental findings of dependence of particle velocity concentration agree with the above analysis.

4. SUMMARY

Grain velocity estimated from cross-correlations of the Photonic probe data, showed an initial increase as solid-concentration increases. Beyond a certain concentration, the velocity decreases due to kinetic energy loss of particle-particle collisions. At a critical threshold of the solid concentration, an incipient condition develops for structural changes in the stream bed morphology. Those structures are initially stripes which may subsequently develop into a meandering structure. An expression was derived for the effect of drag force reduction using a simple model involving similar size particles in a low concentration sediment flow regime. Sedimentary fluid mechanics seems to play a much larger role than thus far has been assumed in sediment transport problems.

REFERENCES

Francis, J.R.D. (1973). "Experiments on the motion of solitory grains along the bed of a water-stream" Proc. R. Soc. London. Ser. A, Vol. 332, pp. 443-471.

Graf, W. H., and Cellino, M. (1999). "Turbulence Suppression in Suspension Flow". In Proc. XXVIII IAHR Congress, Theme D (ed. G. Jirka & B. Manoha). Inst. Hydr. and Hydrol., Tech. Univ. of Graz, Graz, Austria.

Li, M.Z., and Gust, G. (2000). "Boundary Layer Dynamics and Drag Reduction in Flows of High Cohesive Sediment Suspensions", Sedimentology, Vol. 47, pp. 71-86.

Prasad, S.N., Pal, D., and Römkens, M.J.M. (2000). "Wave formation on a shallow layer of flowing grains", J. Fluid Mech. Vol. 413, pp. 89-110.